

# **Technical Report for Final Year (3<sup>rd</sup> Year)**

**on**

**Title of Project: “Development of Ceramics for High Power Lasers”**

**AOARD Grant Number: 09- 4096**

**By Materials Team**

Principal investigator: Akio Ikesue\*

Researcher: Yan Lin Aung\*

\*World-Lab. Co. Ltd., 1-2-19-CSJ308 Mutsuno, Atsutaku, Nagoya 456-0023, Japan.

TEL&FAX:(052)-872-3950

Contact E-mail (PI): [\*\*poly-ikesue@s5.dion.ne.jp\*\*](mailto:poly-ikesue@s5.dion.ne.jp)

**Submission Date: Nov 29<sup>th</sup>, 2010**

**Submitted to**

**Dr. Kumar Jata, Program Manager**

**Asian Office of Aerospace Research & Development (AOARD)**

7-23-17 Roppongi

Minato-ku, Tokyo 106-0032

TEL:(03)-5410-4409 FAX:(03)-5410-4407

[\*\*kumar.jata@aoard.af.mil\*\*](mailto:kumar.jata@aoard.af.mil)

Report Documentation Page			Form Approved OMB No. 0704-0188		
Public reporting burden for the collection of information is estimated to average 1 hour per response, including the time for reviewing instructions, searching existing data sources, gathering and maintaining the data needed, and completing and reviewing the collection of information. Send comments regarding this burden estimate or any other aspect of this collection of information, including suggestions for reducing this burden, to Washington Headquarters Services, Directorate for Information Operations and Reports, 1215 Jefferson Davis Highway, Suite 1204, Arlington VA 22202-4302. Respondents should be aware that notwithstanding any other provision of law, no person shall be subject to a penalty for failing to comply with a collection of information if it does not display a currently valid OMB control number.					
1. REPORT DATE <b>09 FEB 2011</b>		2. REPORT TYPE <b>Final</b>		3. DATES COVERED <b>29-04-2009 to 20-06-2010</b>	
4. TITLE AND SUBTITLE <b>Ceramics for high-power lasers</b>			5a. CONTRACT NUMBER <b>FA23860914096</b>		
			5b. GRANT NUMBER		
			5c. PROGRAM ELEMENT NUMBER		
6. AUTHOR(S) <b>Akio Ikesue</b>			5d. PROJECT NUMBER		
			5e. TASK NUMBER		
			5f. WORK UNIT NUMBER		
7. PERFORMING ORGANIZATION NAME(S) AND ADDRESS(ES) <b>World Lab Co., Ltd.,1-2-19-CSJ308 , Mutsuno, Atsuta-ku,Nagoya 456-0023,Japan,NA,NA</b>			8. PERFORMING ORGANIZATION REPORT NUMBER <b>N/A</b>		
9. SPONSORING/MONITORING AGENCY NAME(S) AND ADDRESS(ES) <b>AOARD, UNIT 45002, APO, AP, 96338-5002</b>			10. SPONSOR/MONITOR'S ACRONYM(S) <b>AOARD</b>		
			11. SPONSOR/MONITOR'S REPORT NUMBER(S) <b>AOARD-094096</b>		
12. DISTRIBUTION/AVAILABILITY STATEMENT <b>Approved for public release; distribution unlimited</b>					
13. SUPPLEMENTARY NOTES					
14. ABSTRACT <b>The ceramic laser gain media fabricated during the 2010 calendar year effort have nearly ideal microstructure. Optical characterizations, using 633 nm laser, showed that the scatter loss is almost zero for the newly fabricated ceramic gain media. The high optical quality of the fabricated ceramics showed high resistance to laser damage when exposed to 1064 nm laser radiation. When used in a laser setup, these devices produced 120 W output power with slope efficiency of 53%. The demonstrated slope efficiency is comparable to that obtained using single crystal and ceramic media obtained from Konoshima. Keywords: Transparent ceramics, transparent polycrystalline material, ceramic laser, high energy laser, high power laser, engineered ceramic composite, waveguide</b>					
15. SUBJECT TERMS <b>ceramic laser, ceramic laser processing, Laser Materials Processing</b>					
16. SECURITY CLASSIFICATION OF:			17. LIMITATION OF ABSTRACT <b>Same as Report (SAR)</b>	18. NUMBER OF PAGES <b>21</b>	19a. NAME OF RESPONSIBLE PERSON
a. REPORT <b>unclassified</b>	b. ABSTRACT <b>unclassified</b>	c. THIS PAGE <b>unclassified</b>			

## Table of Contents

Abstract

1. Introduction	... p.3
2. Objective of the project	... p.4
3. Project schedule and goals	... p.4
4. Fabrication of waveguide laser elements by ceramic composite technology	... P.5
4.1 Simple waveguide laser elements by two-step diffusion bonding	
4.2 Characterization of bonding interface	
4.2.1 Observation under a polarizer (Macro level)	
4.2.2 Transmission polarized optical microscope (Micro level)	
4.2.3 Detecting diffusion distance of Nd after diffusion bonding by SEM/EDS	
4.2.4 Fracture surface comparing with commercial single crystal composite	
5. Laser performance of waveguide laser elements	... P.14
5.1 Side-pump technique	
5.2 End-pump technique	
6. Fabrication of waveguide laser element with long length (L=100mm)	... P.18
7. Conclusions	... P.20

Acknowledgements

## **Abstract**

The ceramic laser gain media fabricated during the 2010 calendar year effort have nearly ideal microstructure. Optical characterizations, using 633 nm laser, showed that the scatter loss is almost zero for the newly fabricated ceramic gain media. The high optical quality of the fabricated ceramics showed high resistance to laser damage when exposed to 1064 nm laser radiation. When used in a laser setup, these devices produced 120 W output power with slope efficiency of 53%. The demonstrated slope efficiency is comparable to that obtained using single crystal and ceramic media obtained from Konoshima.

Keywords: Transparent ceramics, transparent polycrystalline material, ceramic laser, high energy laser, high power laser, engineered ceramic composite, waveguide

## **1. Introduction**

Solid-state lasers (SSLs) are widely used in industrial, medical, and scientific applications such as metal processing, eye surgery, red-green-blue (RGB) light sources in laser printer and projectors, and future nuclear fusion process. Historically, SSLs have utilized single crystal or glass as a laser gain medium. Since the first demonstration in 1964 of continuous wave (cw) laser oscillation in Nd:YAG by Geusic *et al.*, SSLs using single crystal media have continued to mature with power levels increasing to multi-kW levels.

The first laser oscillation using transparent Nd:YAG ceramics was demonstrated by Ikesue *et al.* in the 1990s with laser performance comparable to single-crystal laser oscillation. Recently, ceramic laser technology has emerged as a promising candidate because of its numerous advantages over single-crystal lasers. Perhaps the most important being the ability to produced laser gain media in large size which is not possible using single crystal growth techniques. The development of ceramic laser technology has led to the achievements of compact and highly efficient laser oscillation, ease of control of laser mode, generation of coherence beam with high focusing property. Moreover, the realization of high-power laser based on ceramic technology has brought the visions of ultrahigh-speed machining technology and nuclear fusion one step closer.



## 2. Objective of the project

The objective of the current project has been to develop transparent, low scatter ceramic laser gain media for generation of high output power and high beam quality. Basic technology of ceramic waveguide element, which is controlled with micro-structural refinement and macro- structural design, will be developed, and with the aid of analysis team, laser performances for high power output lasers will be evaluated with related to the thermo mechanical properties of the interface of waveguide designed ceramic laser element.

## 3. Project Schedule and Goals

The three year long project developed transparent ceramic laser media with increasing configuration complexity as shown in Fig. 1. The metric to proceed to the next stage of the development was demonstration of low scatter losses (first using a diagnostic setup and subsequently using the fabricated device in a laser setup). The optical quality and laser performance goals for each stage of the development are summarized in Table 1. For details of the schedule and goals see the reports for YR 1 & YR 2 of the project.

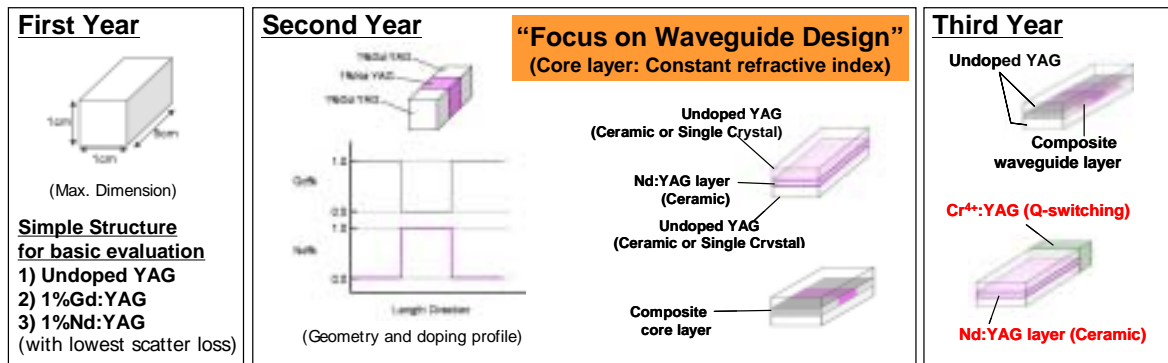


Fig. 1 Laser gain media to be prepared in each year term of the project.

Table 1 Goals for each year term of the project

	Target Laser Output Power
First Year (2008)	Media with lowest scatter loss ( $\sim 10^{-3}/\text{cm}$ )
Second Year (2009)	$\sim 100\text{W}$
Third Year (2010)	300W $\sim$ 1kW

#### 4. Fabrication of waveguide laser elements by ceramic composite technology

In the first and second year terms, it has been already reported that fabrication of high optical quality and low optical loss YAG and Nd:YAG ceramic laser materials were successful, and fabrication of waveguide composite laser elements was demonstrated. In the third year term, the quality of the host materials was further improved by optimizing the synthesis conditions (improvements highlighted in Fig. 2). The improvements in the material quality were determined using a high-resolution TEM (HR-TEM/ EDS) analysis. Newly obtained results are summarized in Fig. 3 (undoped YAG) and Fig. 4 (Nd:YAG).

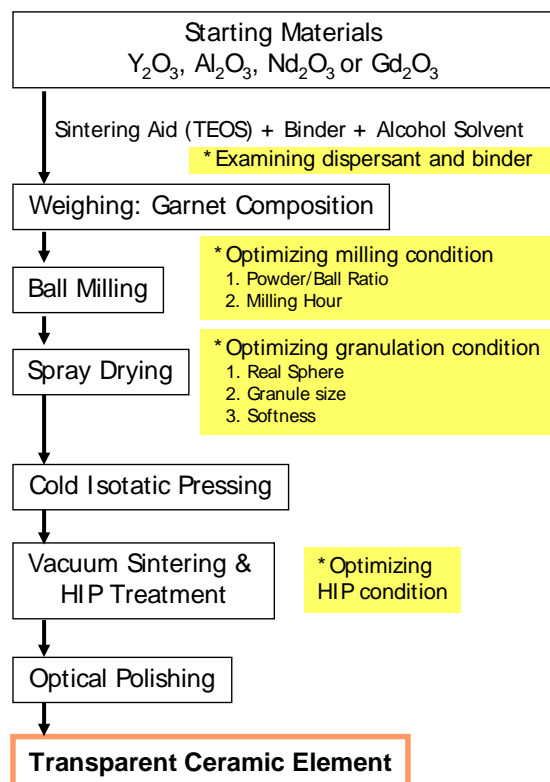


Fig. 2 Fabrication process for the ceramic laser gain media.

It was confirmed that the grain boundaries of high optical ceramic are clean and no grain-boundary phases were observed. According to the EDS analysis results, the detection peaks of internal grain were almost analogous to that of the grain boundary area in both YAG and Nd:YAG ceramic materials. The amount of Si, which was used as sintering aids, was below the detection limit of the diagnostic setup. The data revealed that the optical scattering loss of high quality optical laser ceramics was very similar to that of the single crystal YAG and Nd:YAG. In addition, ceramics with clean grain boundaries can resist high power laser damage.

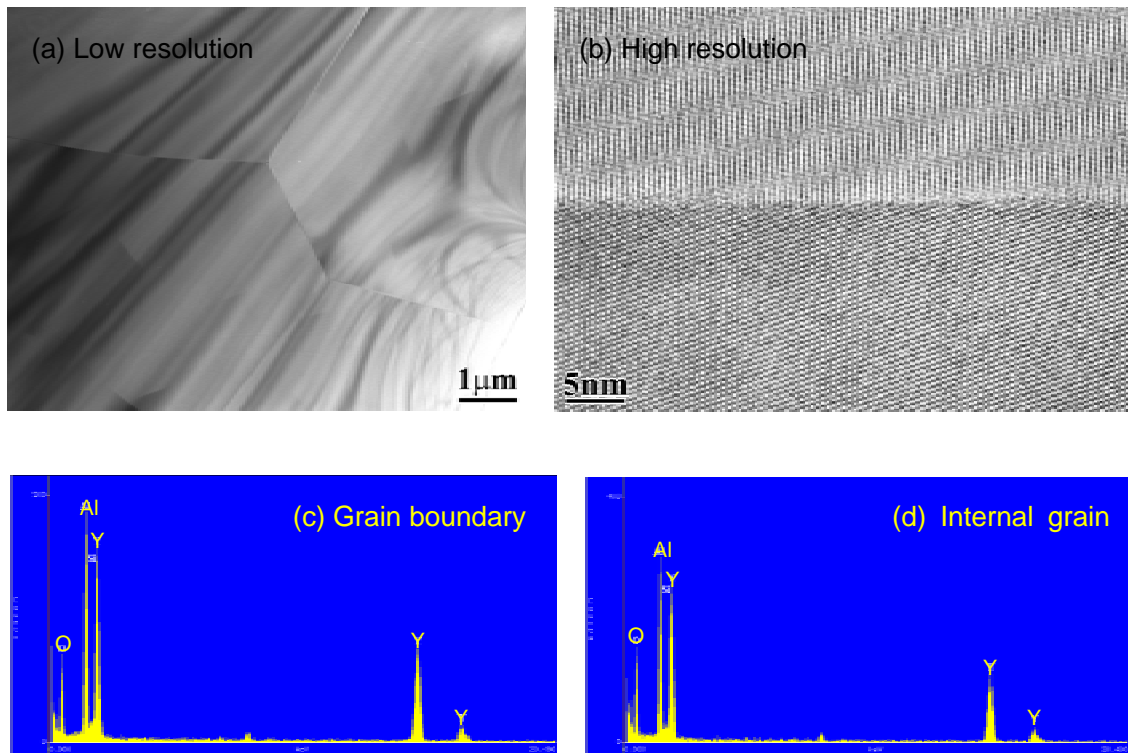
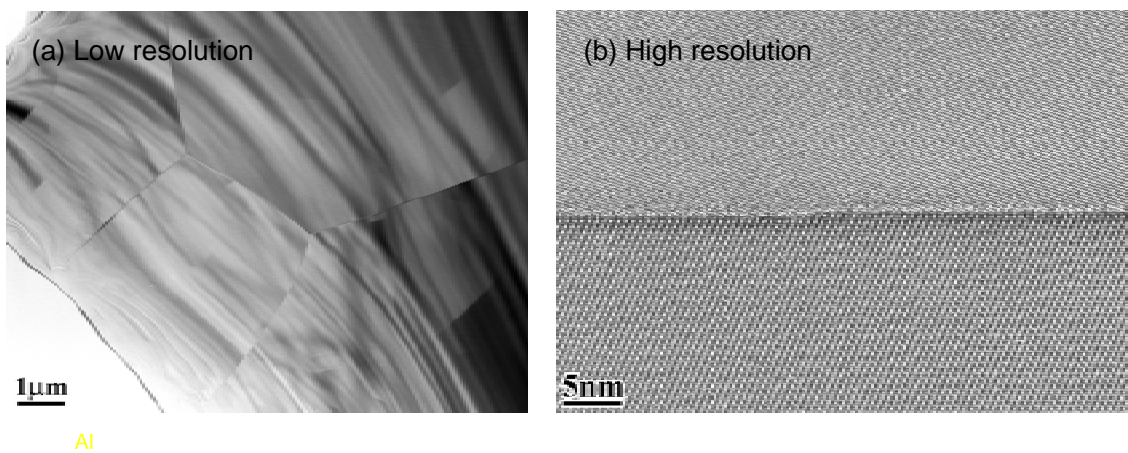


Fig.3 (a) Low resolution TEM image, (b) high resolution TEM image of grain boundary area of high optical quality undoped YAG ceramics. (c) EDS profiles taken at grain boundary and (d) internal grain.



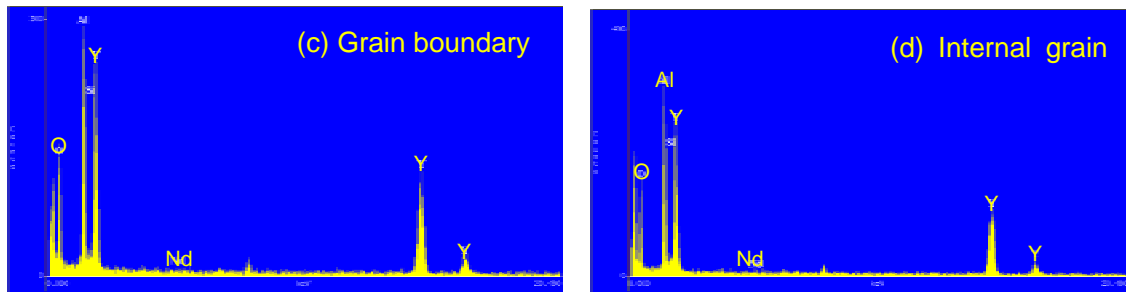


Fig.4 (a) Low resolution TEM image, (b) high resolution TEM image of grain boundary area of high optical quality Nd:YAG ceramics. (c) EDS profiles taken at grain boundary and (d) internal grain.

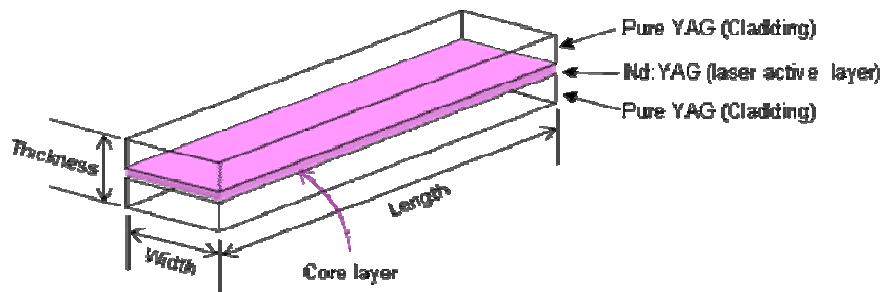


Fig.5 Schematic diagram of Nd:YAG planar waveguide structure.

Based upon the previous achievements, the fabrication effort during the third (final) year emphasized the development of a planar waveguide laser consisting of high optical quality ceramic element with the laser capable of generating  $P_o > 300W$ . The planar waveguide structure (see Fig. 5) consists of a doped active layer (i.e., Nd:YAG) that is cladded between thin layers of undoped YAG to allow for total internal reflection within the doped region. The large surface area inherent to the planar waveguide structure is very effective for cooling and thereby significantly reducing the thermal lensing across the doped region. The planar waveguide is polished on all four narrow regions allowing for pumped longitudinally (for end-pump configuration) or for pumping transversely (for side pump configuration). By applying ceramic composite technology, the Nd doping profile (i.e., the distribution of active ions in the active region) of core waveguide layer can be controlled easier than in the case of single crystal Nd:YAG. Furthermore, it is possible to achieve extremely strong bonding interface that can resist high power pumping. Such kind of bonding interface cannot be realized with high degree of reproducibility when utilizing single crystal waveguide laser elements. The ceramic planar waveguide laser can be expected to generate high output power and with high spatial beam quality.

#### 4.1 Simple waveguide laser element by two-step bonding (Diffusion bonding)

Typical preparation steps for the fabrication of a simple 3-layer waveguide structure are shown in Fig.6. At first, two pieces of undoped YAG (for cladding) and one piece of Nd:YAG (for core layer) ceramics with thickness of around 2mm are prepared. Next, their large flat surfaces are optically polished with a surface finishing better than  $\lambda/10$  at 633 nm. Then the polished surfaces of YAG and Nd:YAG ceramics are contacted and heated at higher temperature for diffusion bonding. A two-layered composite of YAG/Nd:YAG ceramics is obtained.

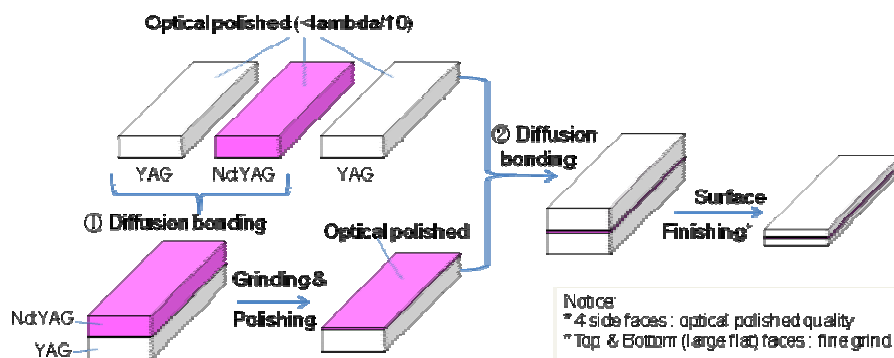


Fig.6 Preparation steps for fabrication of waveguide ceramic laser element.

Then, the thickness of the Nd:YAG layer of the composite is reduced by grinding down until the thickness reaches up to 400 $\mu$ m, and optically polished. The polished surfaces of the Nd:YAG layer of the obtained composite and another piece of optically polished YAG ceramics are contacted and heated at higher temperature for diffusion bonding in order to form a waveguide design. Finally, four side faces are laser polished (to  $\lambda/10$  at 633 nm) and top and bottom surfaces of YAG are ground down until the thickness become 400 $\mu$ m.

In this experiment, waveguide laser elements with two types of Nd:YAG core (0.6 at.% and 1 at.% Nd:YAG) and lengths of 32mm and 62 mm, respectively, were fabricated (see Fig. 7).

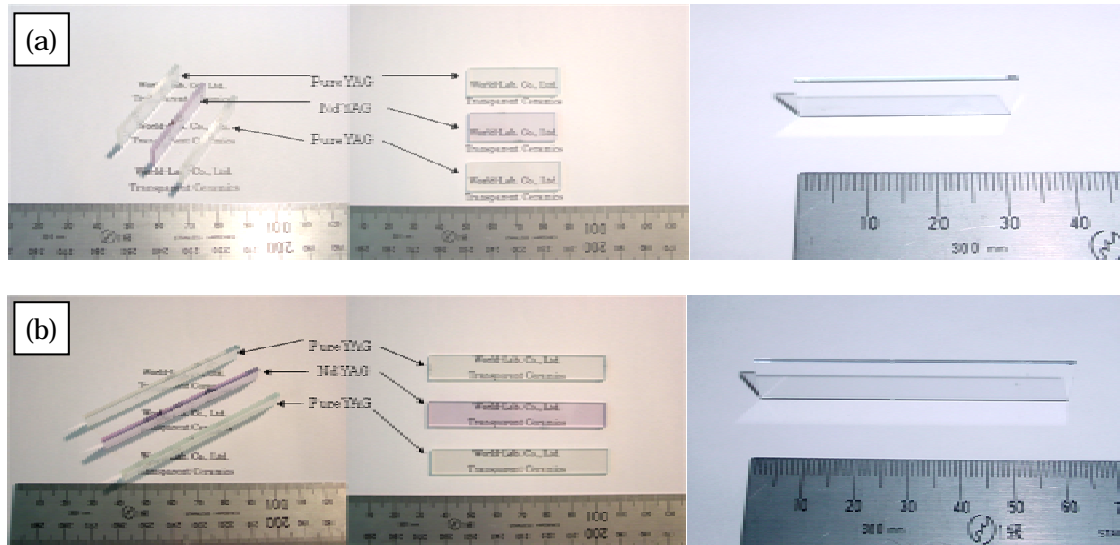


Fig.7 Appearance of optical polished undoped YAG and Nd:YAG ceramic slices before diffusion bonding, and surface finished waveguide laser elements with (a)  $L = 32$  mm and (b)  $L = 62$  mm.

## 4.2 Characterization of bonding interface

In order to examine the basic optical properties of the bonded interface of ceramic waveguide laser elements, fabricated samples were checked under a polarizer, under an optical microscope, and by an interferometry. In addition, the bonded interface was inspected using SEM and line analysis by EDS. For a comparison, fracture property of a commercially available single crystal composite (YAG/Nd:YAG) was compared with a ceramic composite, and their fractured surfaces were observed.

### 4.2.1 Observation under a polarizer (Macro level)

The presence of stress across the bonded interface of the whole sample was studied using a polarizer. As shown in Fig. 8 and Fig. 9, the bonded sample is transparent and only homogeneous color was observed. Abnormal stresses were not observed both in top direction and side direction.

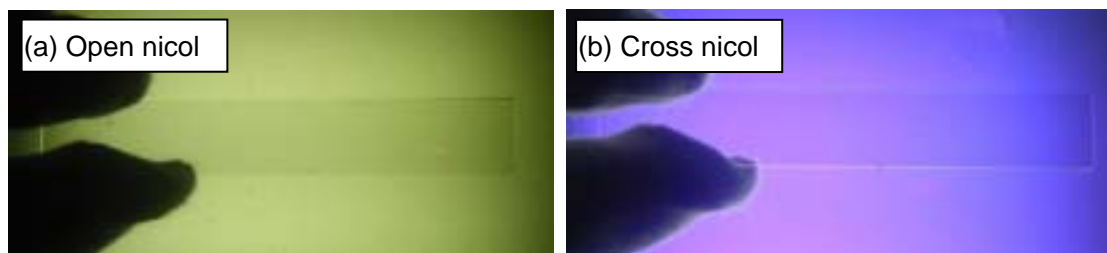


Fig.8. Transmission polarized image of ceramic waveguide element from top view.



Fig. 9 Transmission polarized image of ceramic waveguide element from side view.

#### 4.2.2 Transmission polarized optical microscope (Micro level)

In order to confirm the bonding interface in more details, the samples were inspected under a stereoscopic microscope and a transmission optical microscope. As shown in Fig. 10, both for the 400  $\mu\text{m}$  and the 200  $\mu\text{m}$  core size and, the interstices (poor bonding condition) were not observed. In addition, it was confirmed that the bonding interface of YAG/Nd:YAG composite is free from defects (see Fig.11 also). This suggests that the bonding condition is perfect and its bonding strength is expected to be similar to the host materials.

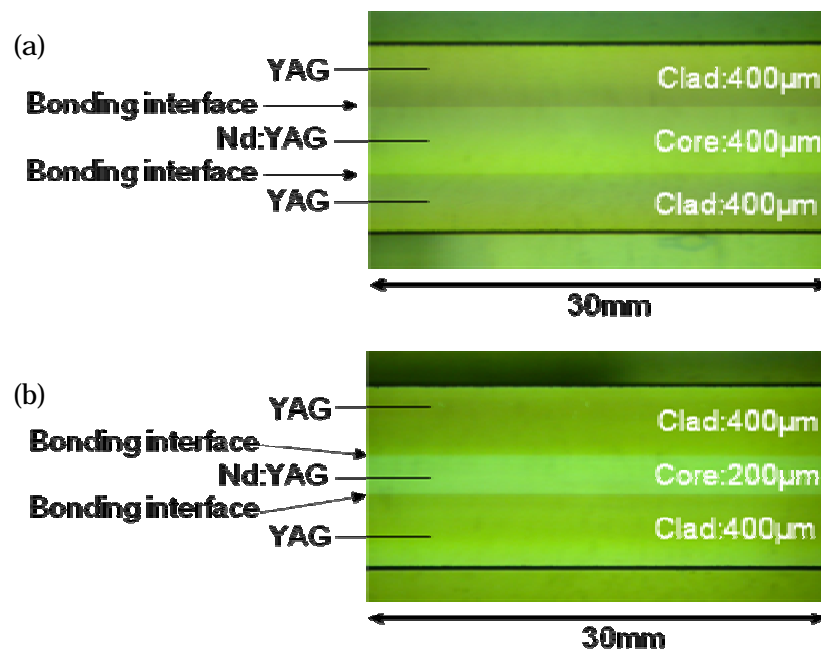


Fig.10 Cross-section of waveguide laser elements under a stereoscopic microscope

(a) Sample with core thickness of 400 $\mu\text{m}$  layer.

(b) Sample with core thickness of 200 $\mu\text{m}$  layer.



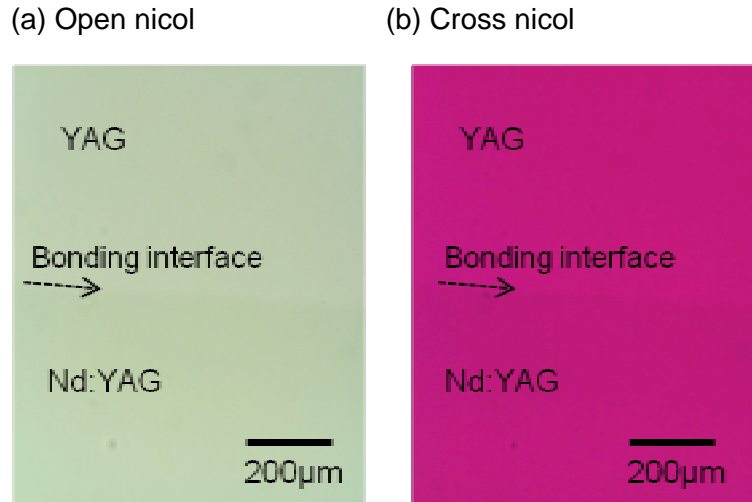


Fig.11 Transmission polarized image of bonding interface of YAG/Nd:YAG composite

#### 4.2.3 Detecting diffusion distance of Nd after diffusion bonding by SEM/EDS

Distribution of Nd elements near the bonding interface was detected by using SEM/EDS analysis. The results are shown in Fig.12. Line scanning was performed along the yellow line across the YAG/Nd:YAG bonding interface. Throughout the scanning area, it was found that the intensities for Al and Y were almost uniform while the intensity for Nd abruptly changed at the distance of 250  $\mu\text{m}$  from the left. It can be assumed that this point is the bonding interface and the diffusion distance of Nd elements was less than 5  $\mu\text{m}$ .

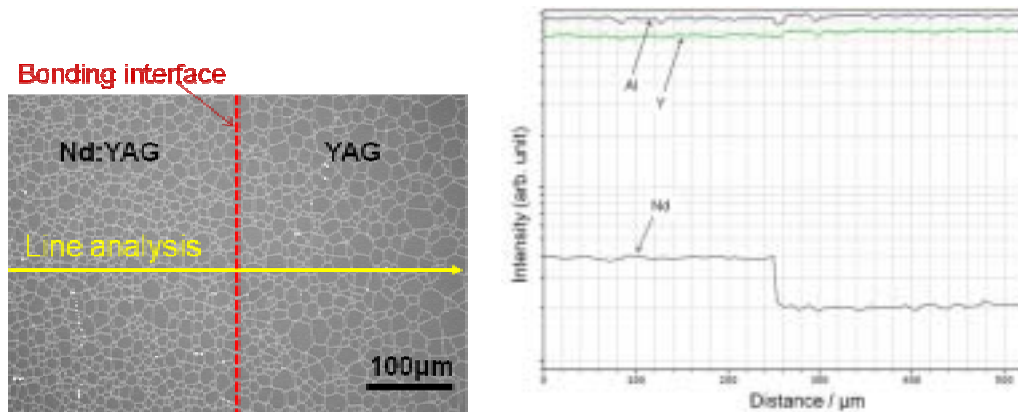


Fig. 12 Microstructure of the Nd:YAG/YAG composite under SEM observation (left) and line analysis results for Nd, Y and Al elements perpendicular to the bonding interface by SEM/EDS (right).



#### 4.2.4 Fracture surface comparing with commercial single crystal composite

Bonding strength of the YAG/Nd:YAG ceramic composite was examined by bending test. A piece of ceramic composite rod, as shown in Fig. 13(a), was prepared by diffusion bonding as same as in the preparation of ceramic waveguide laser elements. Then the sample was broken down by four-point bending. As shown in the picture, the middle of the rod was the bonding interface; however, the fracture occurred at a position apart from the bonding interface. The fracture surface was irregular structure. This showed that the bonding strength is almost very close to that of the host materials and such kind of bonding interface can withstand strong power laser excitation during high power laser experiments.

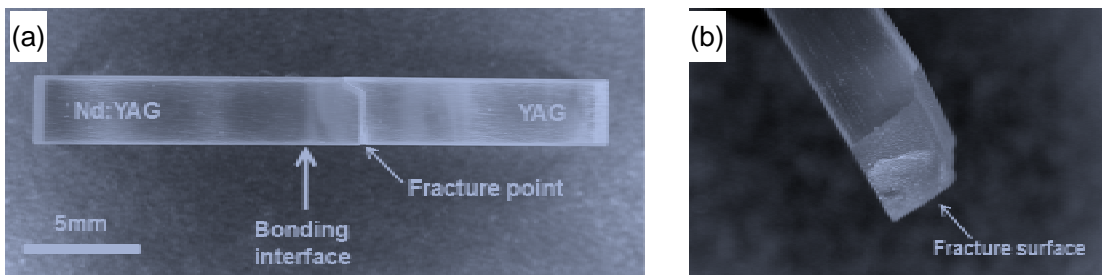


Fig.13 (a) Appearance of fractured Nd:YAG/YAG composite after four-point bending test, and (b) fracture surface of Nd:YAG/YAG ceramic composite materials.

It is also possible to acquire a commercial single crystal composite laser element constituted with YAG and Nd:YAG. Since they have weak bonding strength, those laser elements are limited for low power laser operation. For instance, the commercial single crystal composite can be easily broken by applying a light pressure. A flat surface was observed. This suggests that the bonding strength is weak and the composite is not suited for high power laser operation. Accordingly it was considered that ceramic bonding technology is essential for the development of high power lasers in the future.

## 5. Laser performance of waveguide laser elements

In Fig. 14, photographs of prepared ceramic waveguide laser elements with 0.6 at.%Nd:YAG core are shown. For a comparison, ceramic waveguide laser elements with 1.0 at.%Nd:YAG core were also prepared. Samples with  $L=32\text{mm}$  were for the evaluations of the possibility of the power scaling (side-pump), and samples with  $L=62\text{mm}$  were for evaluations of laser gain (end-pump).

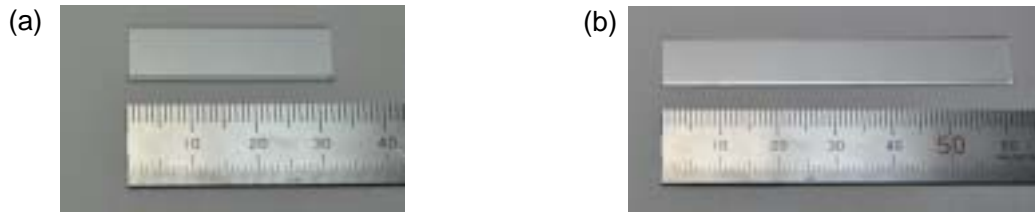


Fig.14 Ceramic waveguide samples with core thickness of  $400\mu\text{m}$  (a), and  $200\mu\text{m}$  (b).

Planar waveguide laser element can generate laser by side-pumping or end-pumping technique. In side-pumping, as shown in Fig.15 (a) and (b), the pump light is injected from the side, i.e., in a direction which is roughly perpendicular to that of the laser beam generation. One of the advantages of side-pumping is, as in (b), that it is possible to pump with several diode bars (side-by-side) from its side faces. Another advantage is that the absorbed pump power can be smoothly distributed in the longitudinal direction. Therefore, it is normally used for power scaling in high power laser generation. An alternate approach is pumping along the laser beam generation direction as shown in (c). It is usually easier to achieve a high gain, good beam quality and high power efficiency with end-pumping, as compared with side-pumping. Disadvantages of end-pumped laser designs are that pump light can be injected only from at most two directions, that the optical intensity and temperature of gain medium vary along the beam direction, and that this approach leads to constraints on the beam quality of the pump source. Therefore, end-pumping sometimes is limited for high-power generation.

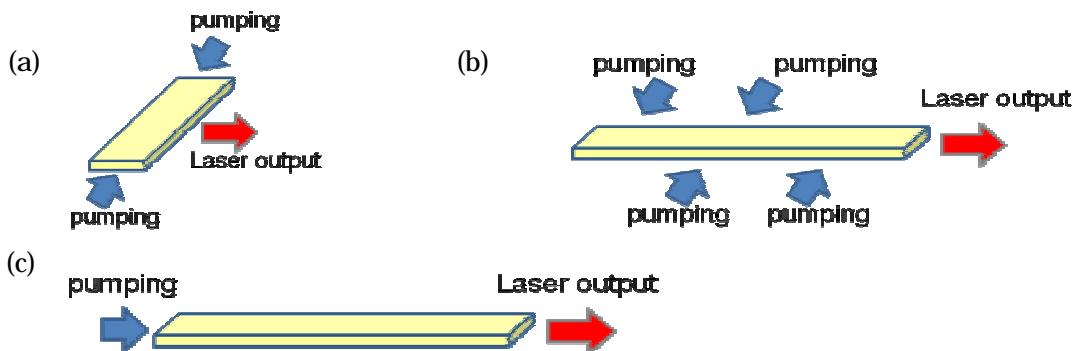


Fig.15 (a)(b) Side pumping technique, (c) end-pumping technique.

## 5.1 Side-pumping

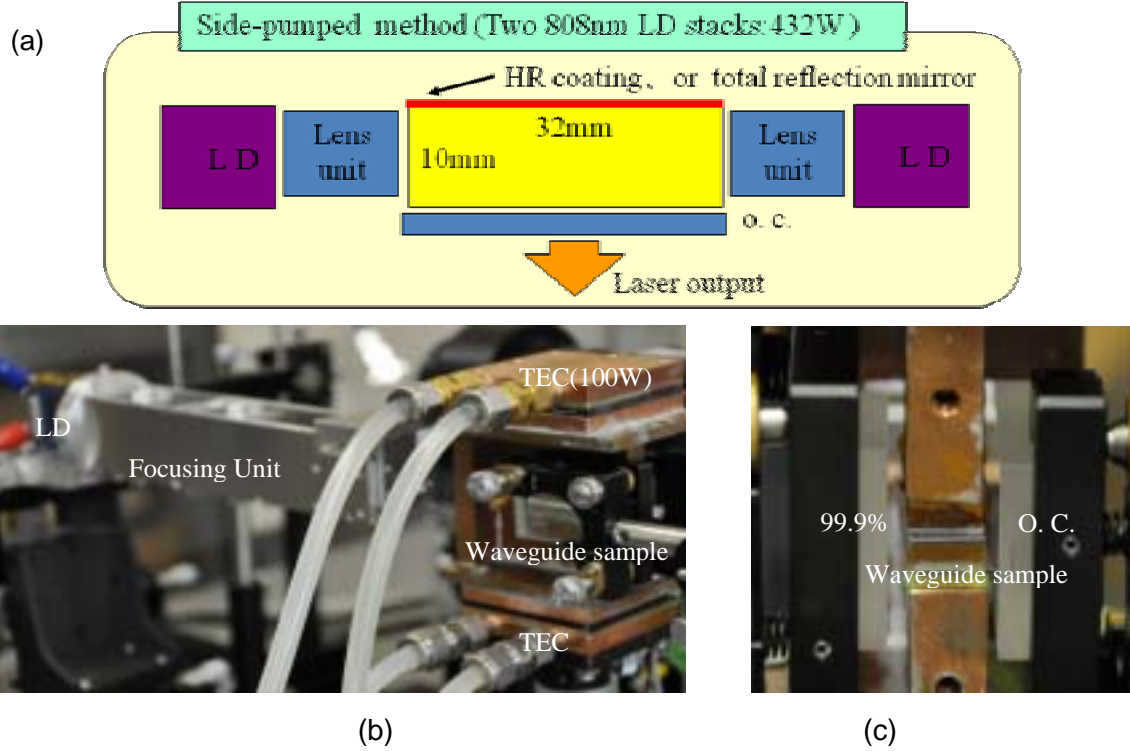


Fig.16 (a) Schematic layout for side-pump laser oscillation experiment, (b) front-view of laser set-up and (c) side-view of the sample holder

A waveguide sample with L32mm was pumped using an LD of wave length 808nm (maximum output 432W) as shown in the schematic layout for side-pump laser oscillation experiment (see Fig. 16). To prevent ASE problem, each side of the sample (10mm x 1.2mm) was taken to have gradient of 3 degree and 4 degree, respectively. Sapphire plates were placed on top and bottom faces of the waveguide sample in order to make pump beam has more total internal reflections. Then the waveguide sample with L32mm was pumped with an LD of wavelength 808nm (maximum output 432W) as shown in the schematic layout for side pump laser oscillation experiment. The thickness of the core of the Nd:YAG was 400 $\mu$ m. AR coating was put for all the edge faces of the sample. Two thermo-electric coolers TEC (100W/ 1 unit) which attached up and down of the sample holder were used for the cooling of the sample. The transmittance of output coupler was set at 20%. Laser performances of 0.6 at.% and 1.0 at.% Nd cores are summarized in Fig.17. In the case of 1.0 at.%, the absorption is much higher than that of 0.6 at.%, and it seems that heat removal was not sufficient in the current set-up. Therefore, 0.6 at.% sample was selected to optimize the laser performance by changing the transmittance of output coupler.

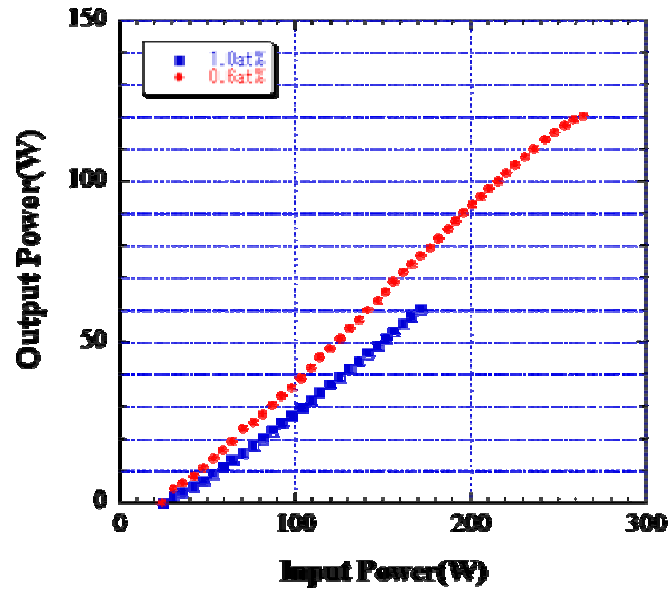


Fig.17 Comparison of doping concentration on output power.

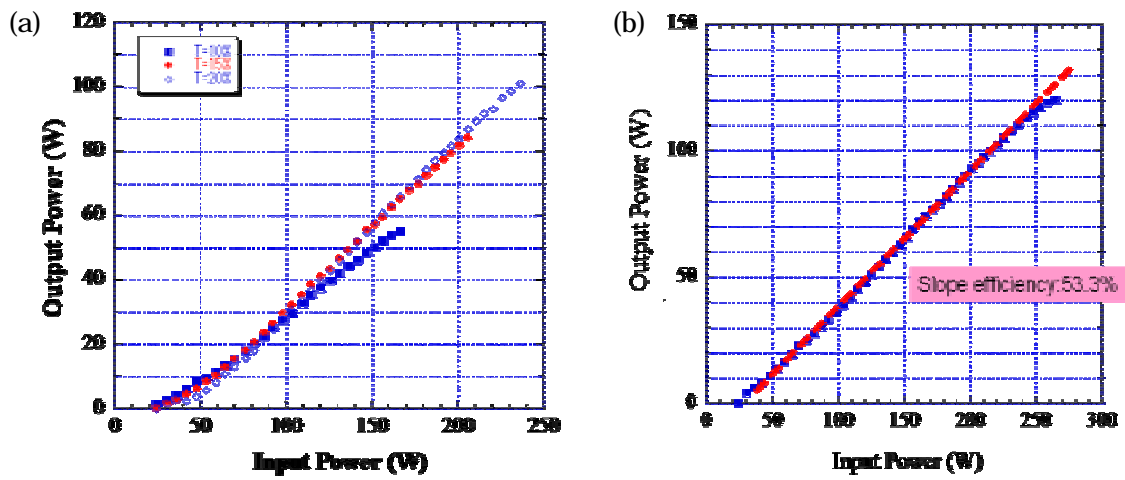


Fig.18 (a) Laser performance at different transmittance of output coupler, and (b) Optimization of the oscillation condition at 20% o. c..

Laser performances at different transmittance of output coupler are summarized in Fig.18 (a). When the transmittance of the o.c. was very low, it seems that more absorbed energy is stored in the gain medium, and saturation of the output power was recognized. From these results, o. c. with 20% transmittance was selected for high power laser oscillation test. Results are shown in Fig.18 (b). Output of 120W was obtained from a sample of Nd concentration 0.6 at%. Over 50% of slope efficiency was achieved. It is considered that the saturation of the output is due to thermal factor, and is not due to the quality of the sample. When pumping with high power from both edges of the sample, temperature distribution was not homogeneous, and this trend became more severe with an increase of higher pumping power. Therefore, higher output power could be expected by introducing a sample cooling system which has more effective cooling power than the current set-up.

## 5.2 End-pumping

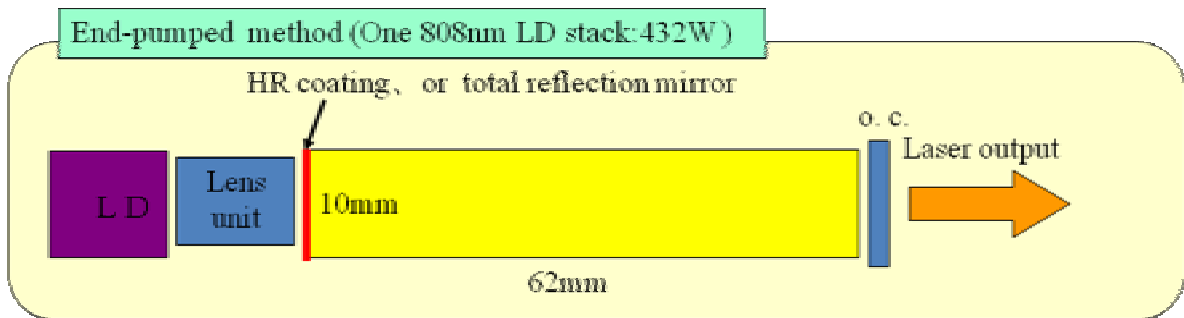


Fig.19 Schematic layout for end-pump laser oscillation experiment,

A waveguide sample with L62mm was pumped using an LD of wave length 808nm (maximum output 432W) as shown in the schematic layout for end-pump laser oscillation experiment (see Fig. 19). The thickness of the core of the Nd:YAG was 200 $\mu$ m. AR coating was put for all the edge face of the sample. Two TEC (100W/ 1 unit) which attached up and down of the sample holder were used for the cooling of the sample. Laser performances of 0.6 at.% and 1.0 at.% Nd cores are summarized in Fig.20. In the case of 1.0 at.%, the absorption is much higher than that of 0.6 at.%, and it seems that heat removal was not sufficient in the current set-up. Therefore, 0.6 at.% sample was selected to optimize the laser performance by changing the transmittance of output coupler. Laser performances at different transmittance of output coupler are summarized in Fig.21. Output of 60W was obtained from a sample of Nd concentration 0.6at%. Slope efficiency was 30% at 40% of O.C.. The cause having lower efficiency of end-pump than side-pump is not understood. Further

comparative experiments are necessary between end-pump and side-pump.

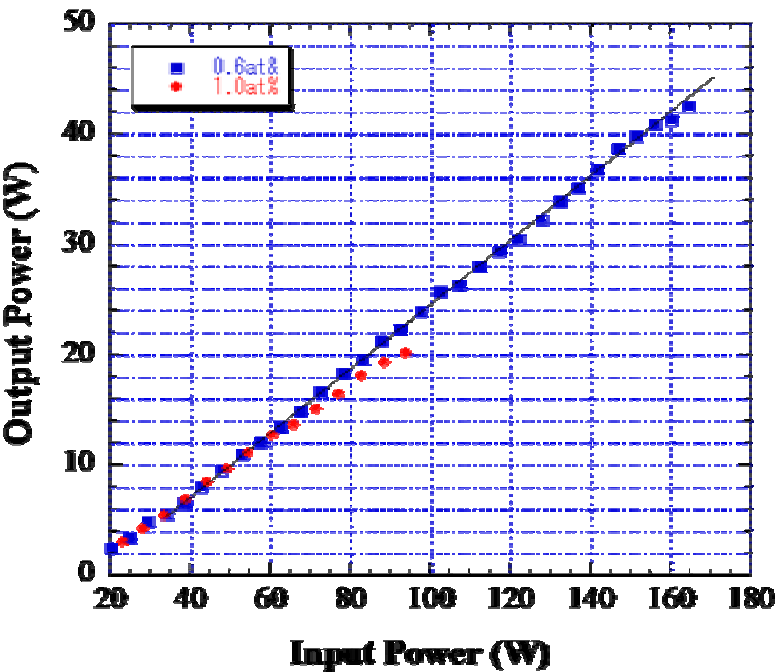


Fig.20 Comparison of doping concentration on output power.

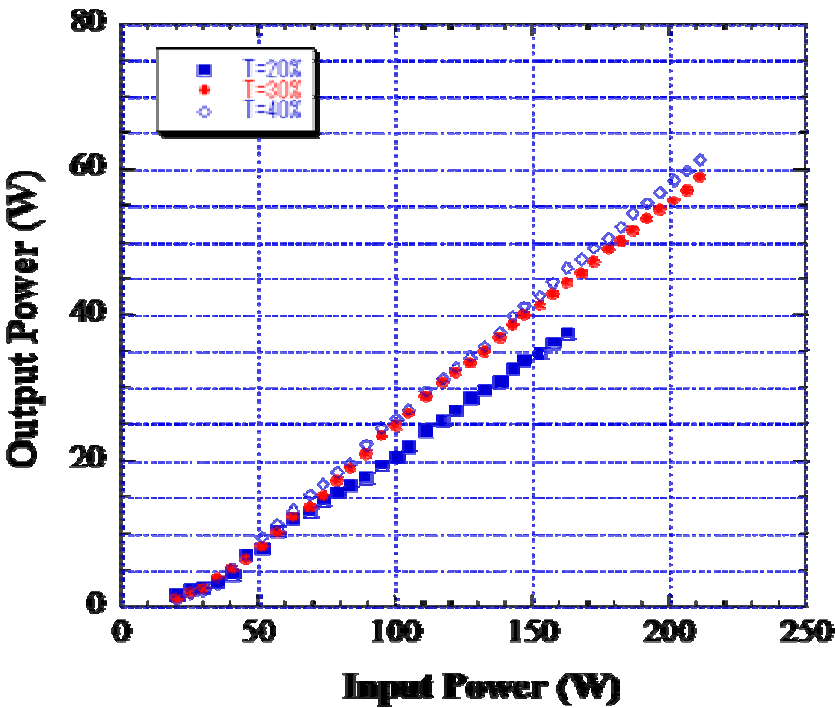


Fig.21 Laser performance at different transmittance of output coupler

## 6. Fabrication of ceramic waveguide laser element with long length (L=100mm)

To achieve higher output power, waveguide laser element with longer length is required. The long direction can use pump beam effectively (high-gain and high-efficiency). Output power of 1kw or more (slope efficiency over 50%) could be expected from the waveguide structure (dimension: for example, larger than W20mm x L100mm).

Fabrication of large scaled ceramic waveguide laser elements was also demonstrated. Preparation steps similar to that of the previous short waveguide samples were applied also for this case. However, it was not possible to make a waveguide laser element with perfect bonding condition.

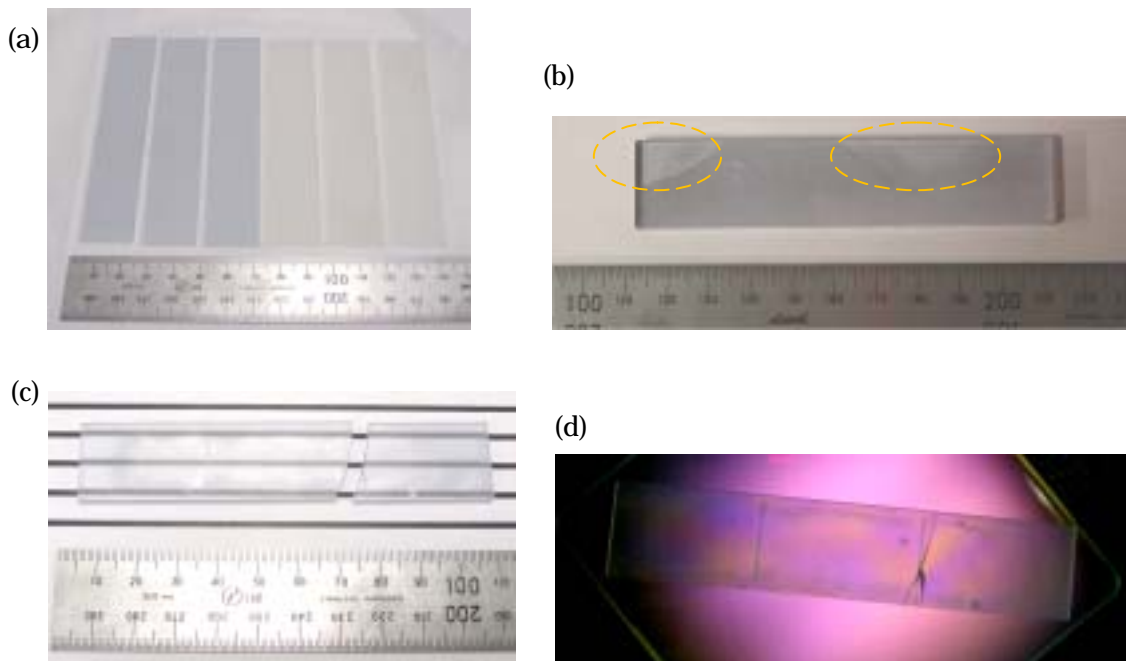
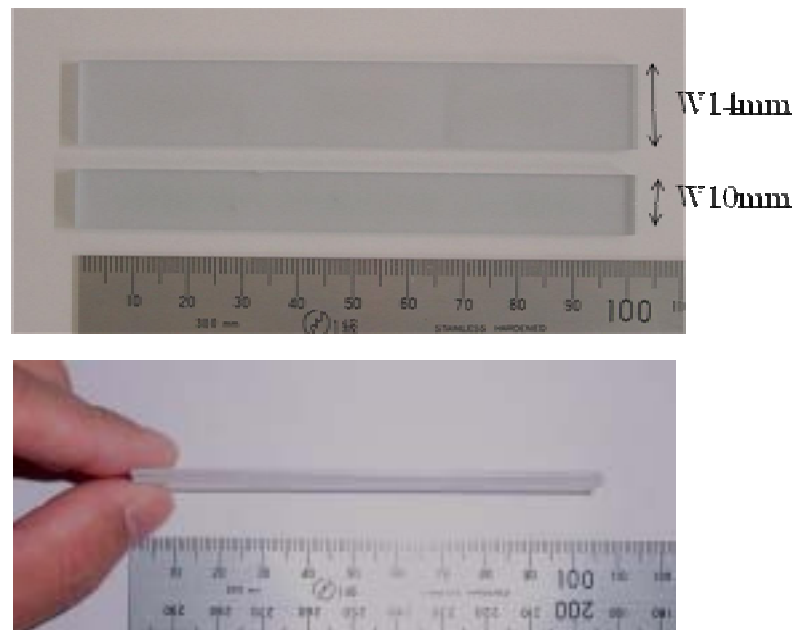


Fig.22 (a) Optical polished undoped YAG and Nd:YAG before diffusion bonding. (b) Waveguide sample prepared with almost pressure less condition. (c) Waveguide sample prepared under very high pressure. (d) Internal stress condition of the waveguide sample prepared under very high pressure.

Some typical failures are shown in Fig. 22. When the large sample (W20 x L100mm) was prepared at almost pressure less condition, some non-bonded areas (yellow circles in (b)) were observed in the sample by naked-eyes. On the other hand, when it was prepared under very high pressure condition, the sample was broken, and when it was observed under a polarizer, the whole sample was suffered with mechanical stress. It

was difficult to achieve a waveguide sample with  $W=20\text{mm}$ . Therefore, to make easier, fabrication of waveguide samples with  $W=10\text{mm}$  and  $14\text{mm}$  was carried out with modified bonding condition. Finally, it was successful to make waveguide samples with  $W10 \times L100\text{mm}$  and  $W14 \times L100\text{mm}$ . Their photos are shown in Fig. 23. There was not enough time and facilities to demonstrate laser oscillation using those samples during the period of this project. But we will find next opportunities to evaluate the laser performance of those samples in the future.



Fig, 23 Photographs of waveguide samples with  $W10 \times L100\text{mm}$  and  $W14 \times L100\text{mm}$ ,



## 7. Conclusions

In this project, the key point was to produce ceramic laser gain media with extremely low optical loss ( $10^{-3}/\text{cm}$ ) which is comparable to the Konoshima's ceramics and commercial single crystal counterparts. Additionally, it was to generate high output power laser (over 100W to 1kW level) from a ceramic laser gain medium focusing on planer waveguide design.

In the first and second year terms, it was succeeded to produce high optical quality ceramic laser materials (optical loss:  $<10^{-3}/\text{cm}$ ) with reliable reproducibility. Their basic optical and physical properties were investigated from macro-, mirco- to atomic level. It was shown that high optical ceramic materials have clean grain boundaries, no secondary phase or grain boundary phases, no optically inhomogeneous phases (no inclusions), and no residual pores. In addition, HR-TEM and EDS analysis results revealed that the fabricated ceramics have almost an ideal and perfect microstructure (no atomic defects were observed). Due to the formation of an ideal and perfect microstructure, scattering loss of the high quality ceramics was as low as a commercial single crystal counterpart, and it showed very high resistance to high energy laser damage. Laser performance with very close to theoretical quantum efficiency was achieved from the developed high quality ceramic gain media, comparable to that of the Konoshima's ceramics and also commercial single crystal counterpart.

In the third year term, fabrication of ceramic composite with planar waveguide structure (Nd:YAG core layer is sandwiched with undoped YAG cladding) was focused for the generation of high power laser. It was verified that the perfect bonding interface formed by ceramic composite technology has a bonding strength which is comparable to that of host materials, suggesting that such kind of bonding interface is essential for the development of high power lasers in the future. By using a ceramic waveguide laser element, it was possible to achieve output over 100W from a volume of  $400\mu\text{m} \times 10\text{mm} \times 32\text{mm}$ , which is almost equivalent to  $\sim 1\text{kW}/\text{cm}^3$  level. This output power was not limited by the quality of the ceramic waveguide but because there was no enough time and facilities to generate higher output during the period of this project.

Thanks to the achievements from this project, fabrication of large scaled ceramic waveguide laser elements has become available, and development of high power laser will be speed up to obtain more excellent results in the near future.

**LIST OF MANUSCRIPTS SUBMITTED OR PUBLISHED UNDER AFOSR/AOARD  
SPONSORSHIP DURING THIS REPORTING PERIOD:**

A part of the project was slightly introduced in the following publication (review article).

1. Akio Ikesue and Yan Lin Aung, "Ceramic laser materials", Nature Photonics, VOL.2, December (2009) [www.nature.com/naturephotonics](http://www.nature.com/naturephotonics)

**Acknowledgement**

This work was supported by AFOSR/AOARD through funds received from Roppongi office, Tokyo AOARD Grant Number: 09- 4096.